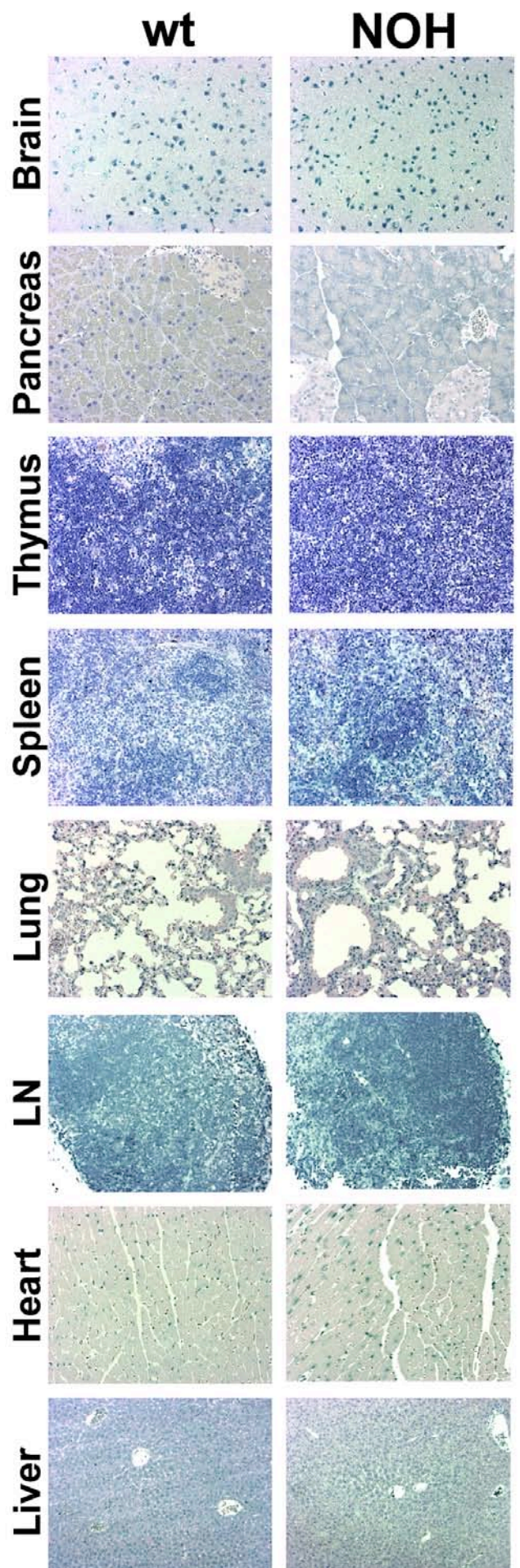


**Supplemental Figure 1:**

**A. Lack of OVA expression in tissues other than kidney glomeruli (to the right).**

A. Sections of various tissues of NOH (left) and non-tg control (right) mice were stained for OVA expression by the same technique used in Figure 1B. Red= OVA, blue=nuclei. Original magnification x1000.



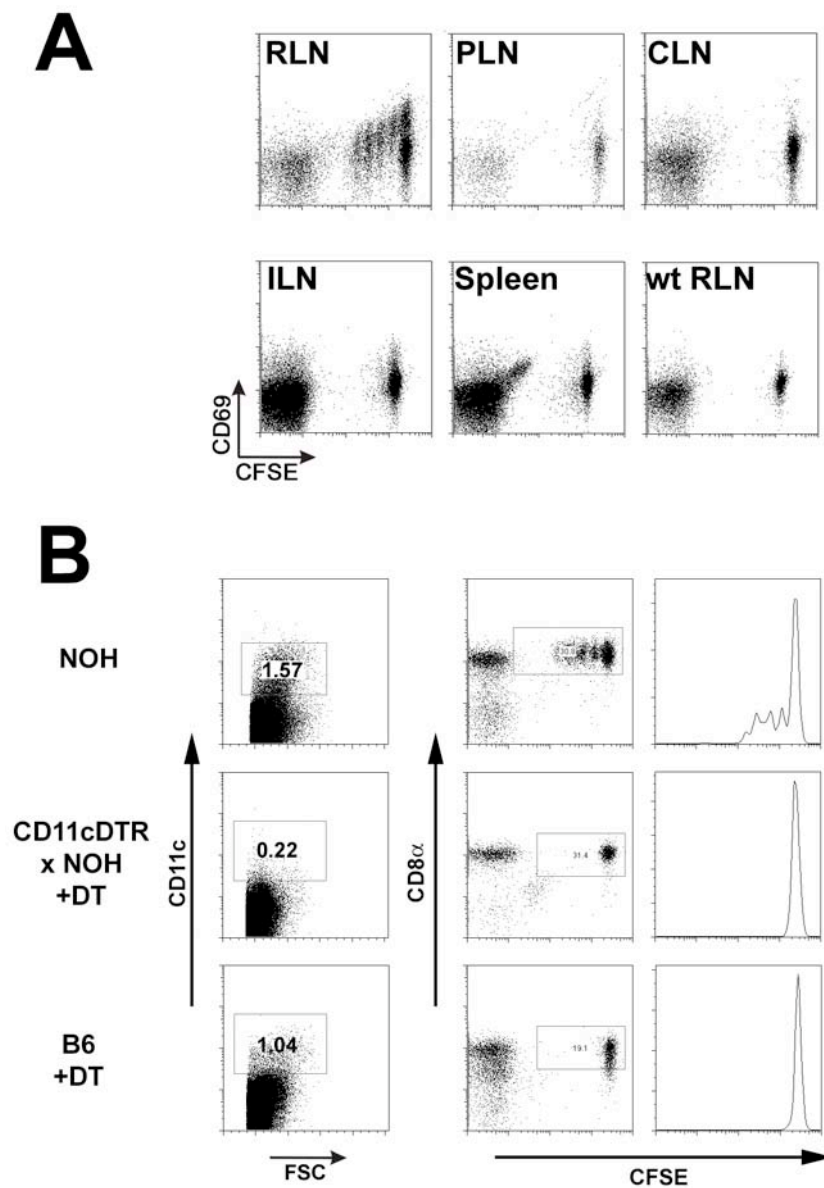
## Supplemental Table 1

### Quantitative RT-PCR of tissues of NOH mice (below)

Tissues were snap frozen in liquid nitrogen and homogenized in Trizol. Proteins were removed by phenol/chloroform extraction and nucleic acids were purified by Ethanol precipitation. DNA was removed by DNaseI digestion (New England Biolabs) for 15 min followed by inactivation for 10 min at 75°C. RNA was quantified by Nanodrop (Thermo Scientific) to ensure equal amounts of RNA for cDNA synthesis, which was done by Superscript II reverse transcriptase (Invitrogen). PCR was performed on a Light Cycler<sup>®</sup> 480 detection system (Roche) as follows: initial denaturation 95°C for 5 min, followed by 50 cycles of: 95°C 10 sec, 60°C 30 sec, 72°C 1 sec. Probes were from universal probe library (Roche); OVA primers GTGTTTAGCTCTTCAGCCAATCT and CTGCATGGACAGCTTGAGATA; PGK1 primers TCTAGGGGTTGCATCACTATCA and TTCCATTTGGCACAGCAAG. The 2<sup>nd</sup> and 3<sup>rd</sup> column indicate the first PCR cycle when a signal for OVA or PGK1 was detected.

Organ	PCR Cycles	
	OVA	PGK1
<b>Kidney</b>	40,01±0,29	24,34±0,07
<b>Liver</b>	>50 (n.d.)	25,38±0,12
<b>Brain</b>	>50 (n.d.)	23,56±0,04
<b>Pancreas</b>	>50 (n.d.)	26,16±0,17
<b>Spleen</b>	>50 (n.d.)	24,38±0,07

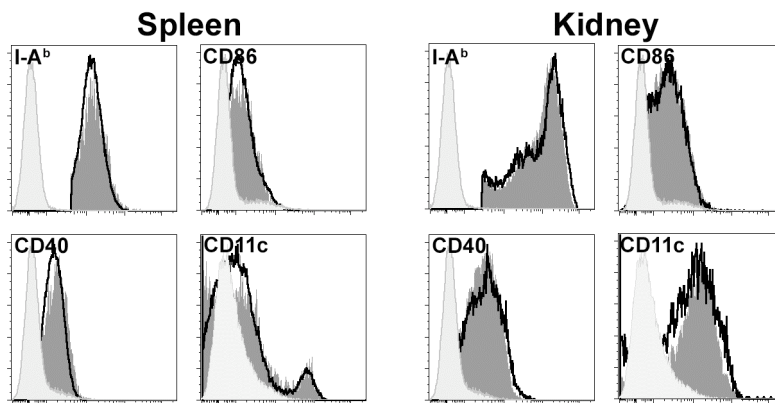
Supplemental Figure 2:



**DCs cross-present glomerular antigen in the renal lymph nodes.**

(A)  $2 \times 10^6$  CFSE-labeled OT-I T cells were isolated from LNs and spleen of NOH and wt mice on d3 after adoptive transfer. CD69 was measured as early T cell activation marker. Data are representative of 3 individual experiments in groups of at least 3 mice. (B) Proliferation dot plots and histograms of OT-I cells isolated from similar to A of NOHxCD11c-DTR or wt mice injected with DT to deplete DC on the day of adoptive T cell transfer. DC depletion was confirmed by staining splenocytes for CD11c<sup>+</sup> cells on d3. Results are representative for the results shown in Figure 1A-E.

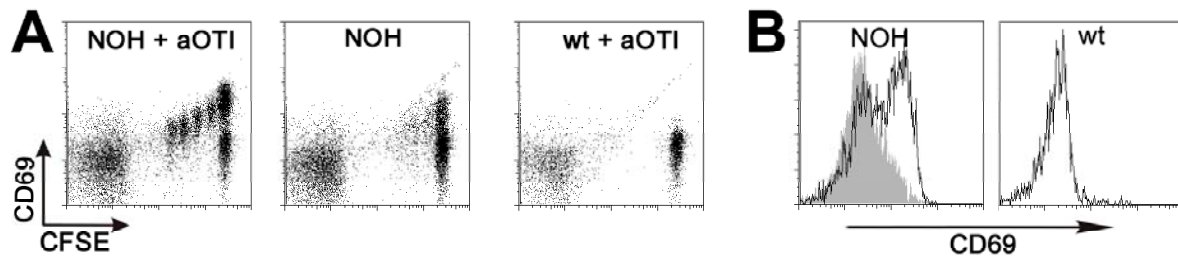
**Supplemental Figure 3:**



**Splenic and renal DCs from NOH and wt mice show the same activation state.**

DCs isolated from the spleen (left) and kidneys of NOH mice (thick line) and wt controls (dark grey area) were stained for MHC class II (I-Ab), CD86, CD40 and CD11c or left unstained (light grey areas). Expression levels are given as overlays in histograms.

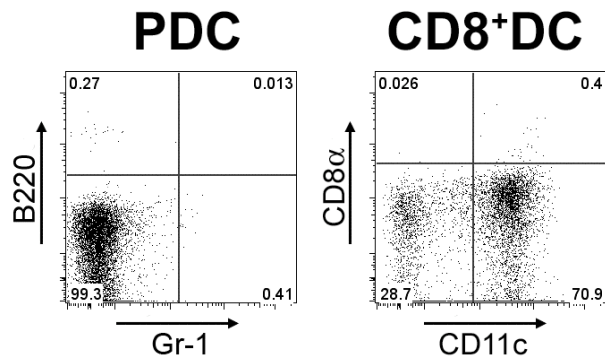
**Supplemental Figure 4:**



**Activated OT-I cells enhance priming of naive OT-I T cells.**

(A) Proliferation and CD69 expression of CFSE-labeled OT-I cells in the renal lymph nodes of NOH and wt mice after challenge with *in vitro* activated OT-I cells. Data are representative of 2 individual experiments in groups of 3 mice. (B) Histograms of CD69 expression on adoptively transferred OT-I of unchallenged (filled histogram) or OT-I challenged (empty histogram) NOH mice compared to wt mice. Results are representative for the results shown in Figure 2A, B.

**Supplemental Figure 5:**

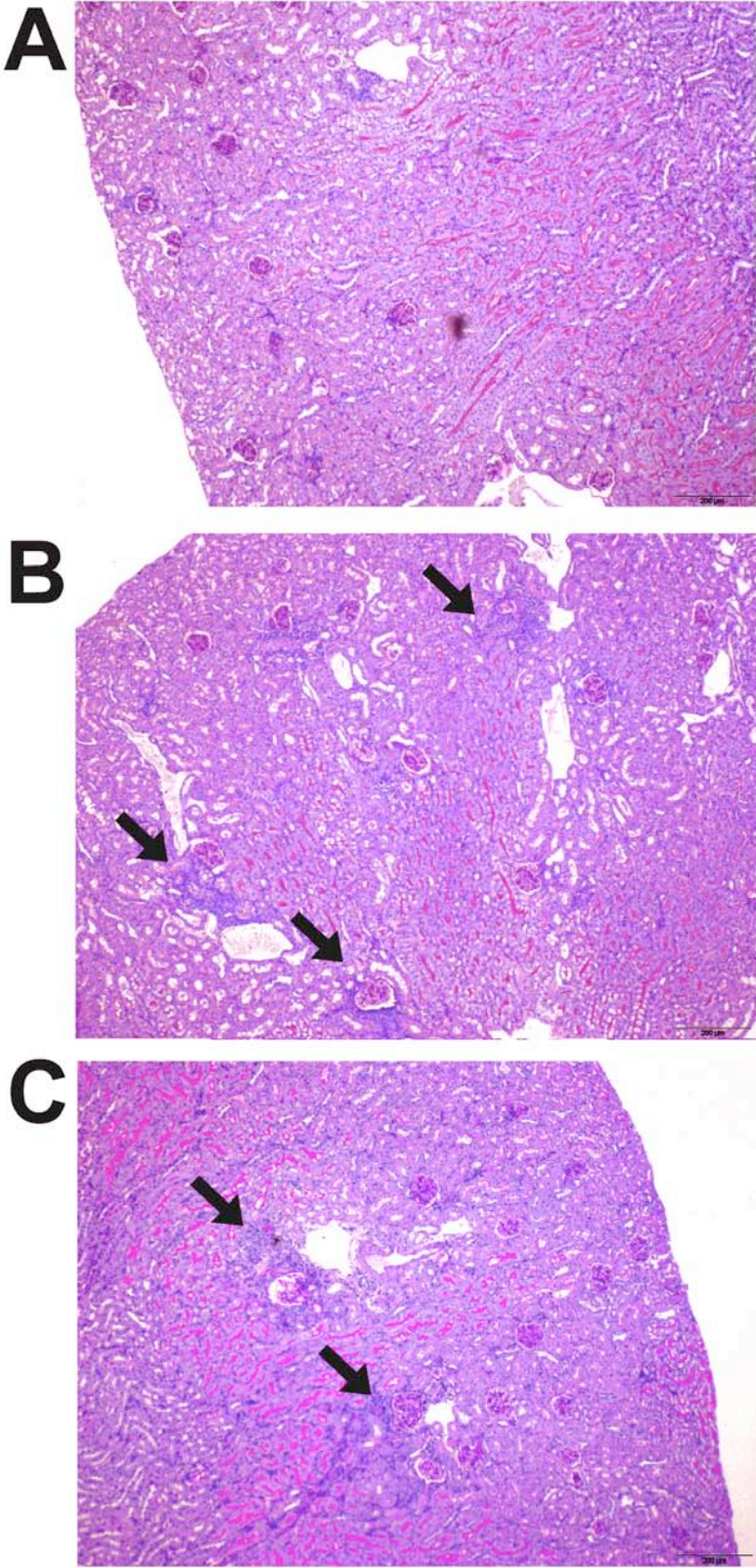


**Kidney infiltrates contain neither plasmacytoid DC, nor conventional CD8<sup>+</sup> DC.**

Kidney single cell suspensions of NOH mice on d7 after OT-I/a-OT-II cell transfer were gated for CD11c<sup>+</sup> MHC II<sup>+</sup> DCs and stained for Gr-1 and B220 to identify plasmacytoid DCs (left dot-plot), and gated for MHC II<sup>+</sup> cells and stained for CD11c and CD8α to identify conventional CD8<sup>+</sup> DC (right dot plot).



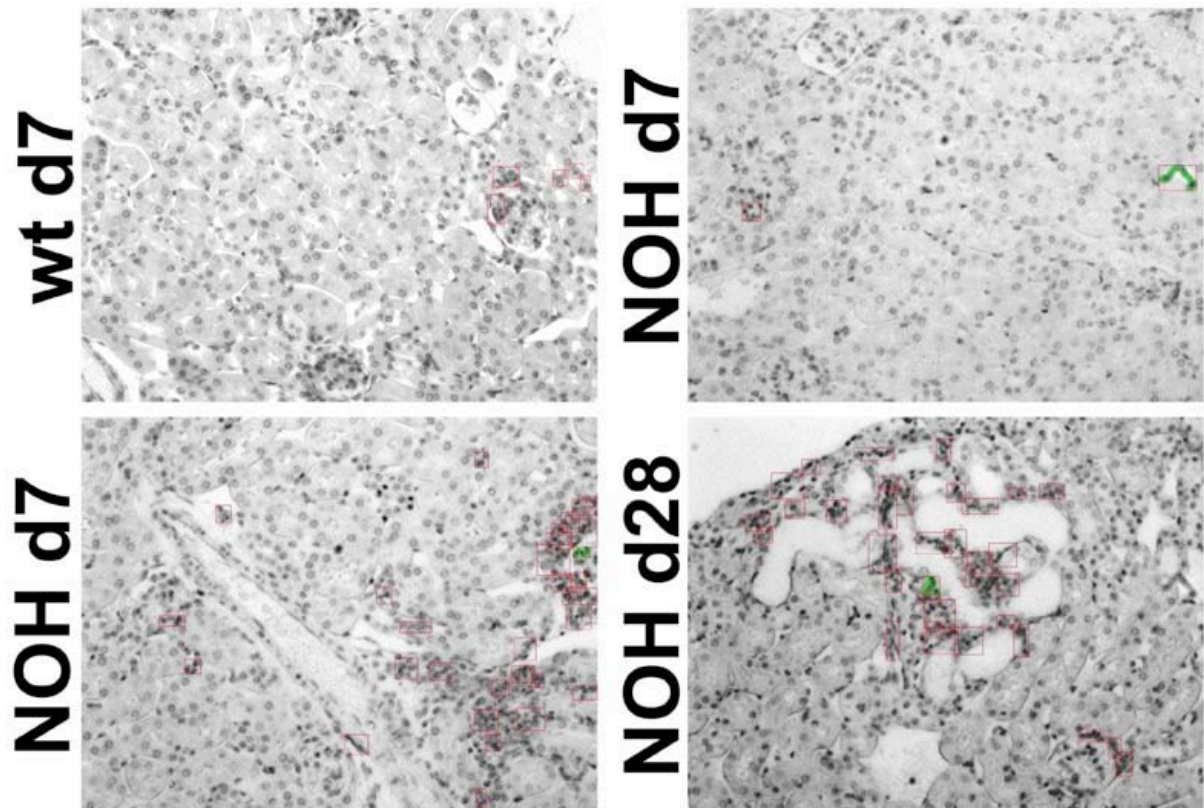
Supplemental Figure 6:



**Large overview of periglomerular infiltrates after DC depletion**

These images give a larger overview over kidneys of NOH x CD11c-DTR (A, B) or NOH mice (C) injected with DT (A, C) or not (B) as described in Figure 5.

**Supplemental Figure 7:**

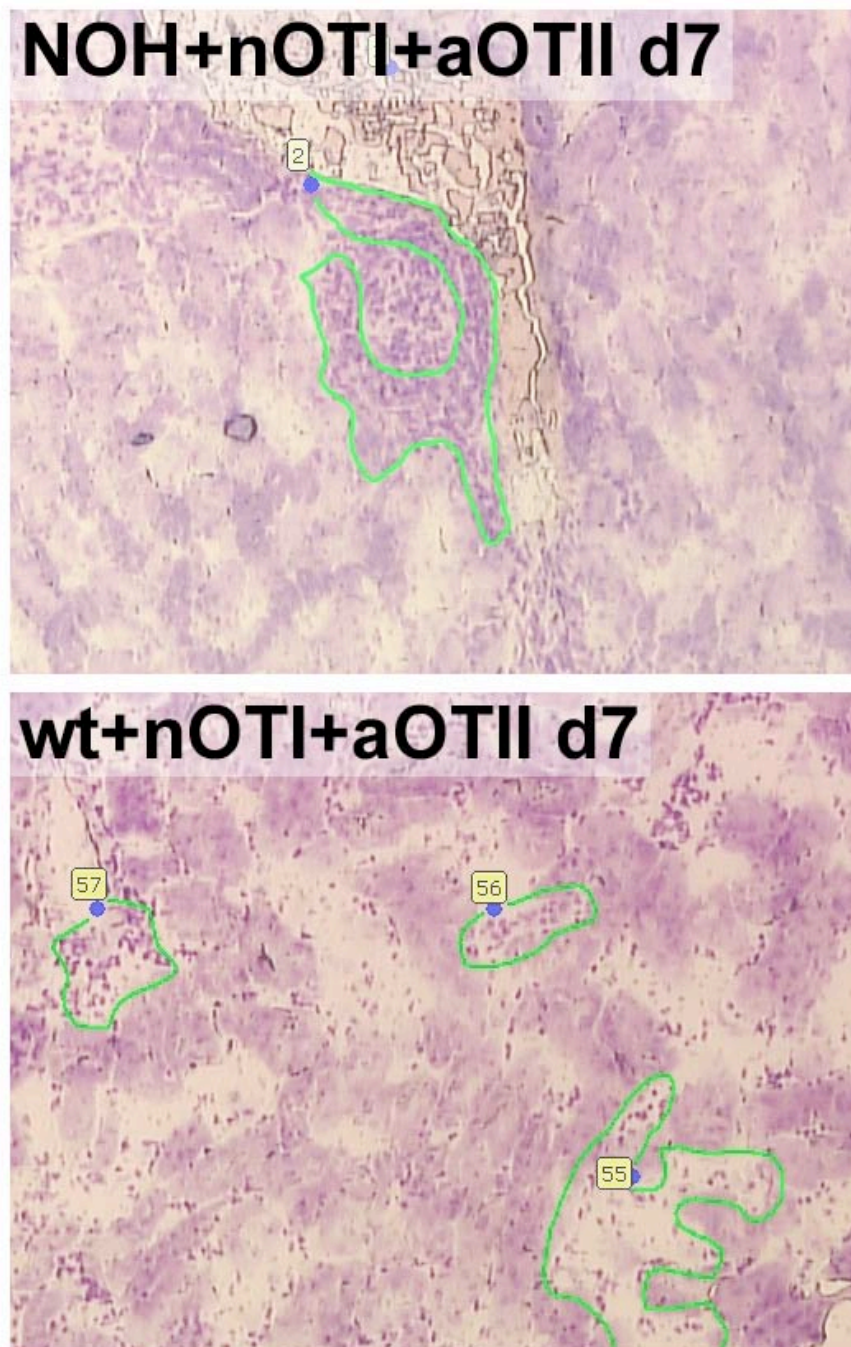


**Example of automated quantitative analysis of periglomerular infiltrates**

Typical individual images (434x330  $\mu\text{m}$ ) are shown as an example for quantitative analysis of infiltrates using ScanR software. All pictures were taken from mice that had received  $5 \times 10^6$  naïve OT-I and  $5 \times 10^6$  OT-II cells. Upper left panel: wt mouse. Upper right panel: uninfiltated area of a NOH mouse on d7, where the software did not detect infiltrates. Lower left panel: infiltated area of NOH mouse d7. Lower right panel: infiltated area of NOH mouse d28. Red boxes indicate clusters detected by the software. Original magnification x20.



**Supplemental Figure 8:**



**Excision of periglomerular infiltrates by tissue laser microdissection**

Glomeruli were excised from cresylviolet-stained kidney cryosections using a PALM MicroBeam IP 230V Z microscope for laser pressure catapulting (P.A.L.M., Bernried, Germany). Subsequently, periglomerular infiltrates (upper panel) were cut out for isolation of mRNA as indicated by the green lines. Similarly sized tubulointerstitial areas were isolated from non-infiltrated kidneys as control (lower panel).